Contents

1 Supplementary Methods

1.1 Participants

We used data from the Social and Health Impact of Network Effects (SHINE) study, a larger study designed to provide insight into health behaviors and social interactions among young adults. Eligible social groups included on-campus organizations containing 20-100 members, with at least 80% of the members interested in participating in the study. Of eligible social groups, 925 individuals were invited to enroll in the study. These individuals were from 24 social groups across the two universities (33% performing arts groups, 29% sororities or fraternities, 25% sports clubs, 8% technology clubs).

1.2 Eligibility criteria

Participants were eligible to enroll in the study if they were a member of one of the social groups invited to participate. Those who were willing to participate were invited to complete the baseline survey. Eligibility for the MRI session was determined by participant responses to questions in the baseline survey and the response completion rate of the social group. Social groups were eligible if more than 15 people completed the survey or if more than 20% of the group members completed the survey. Based on these criteria, 19 social groups were eligible. Of these groups, individuals were eligible to complete the MRI session if they: were 18 years or older, fluent in English, and free from MRI contraindications; weighed less than 350 lbs; were not claustrophobic, pregnant, or studying abroad at the time; had no history of serious medical issues, psychiatric hospitalization, or drug abuse; and drank alcohol and listed at least two people in their social group who drank the least in the group apart from themselves. Of the participants who completed the baseline survey 113 participants were invited to complete the MRI session.

One participant was deemed ineligible for the MRI scan due to a contraindication discovered at the session, but they completed all behavioral components of the session. Another participant was scanned but the data was lost due to a technical error. This yielded a total of 77 participants in the mindful ($n = 38$) or baseline ($n = 39$) groups.

1.3 Group assignment

Participants who enrolled in the MRI session component were randomly assigned to one of three intervention groups: mindful attention, perspective-taking, or baseline. In the mindful attention and perspective-taking groups, participants were trained to use cognitive strategies to regulate their responses to alcohol cues. The baseline participants was instructed to respond naturally without trying to alter their responses. In this paper, we focused on investigating the effects of mindful attention compared to the baseline condition.

1.4 MRI data acquisition

Scans were acquired using 3-Tesla Siemens Prisma scanners equipped with a 64-channel head coil. For each participant, scans were acquired in the following sequence: a resting-state scan, two runs of a face perception ("faces") functional MRI (fMRI) task, a T1-weighted structural scan, four runs of a cue-reactivity fMRI task, a fieldmap for the diffusion-weighted (DWI) scan, a diffusion-weighted (DWI) scan, and a T2-weighted structural scan. DICOM images were converted to NIfTI files in the Brain Imaging Data Structure [1] format using HeuDiConv [2]. The DWI data were preprocessed and reconstructed through QSIprep (Version 0.8.0; [3]). Briefly, the data was first denoised and bias corrected, and then underwent susceptibility distortion correction, as well as motion and eddy current correction via FSL 6.0, and were coregistered to the T1 space. We also warped both the Schaefer atlas [4] and the Harvard Oxford subcortical atlas [5] into individual T1 space to subdivide the brain into 400 cortical and 14 subcortical regions. Then, the preprocessed DWI data was reconstructed using generalized Q-sampling Imaging [6] in DSI-Studio (http://dsi-studio.labsolver.org). Deterministic tractography [7] was performed until 5×106 streamlines were reconstructed, yielding individual structural networks with brain regions as nodes and the number of streamlines connecting each brain region pair as weighted edges. Preprocessing was performed using QSIPrep (Version 0.8.0), which is based on Nipype (Version 1.4.2; [8]).

1.5 Anatomical data preprocessing

The structural, resting-state, and task-based fMRI scans were preprocessed using fMRIPrep (Version 20.0.6; [9]), which is based on Nipype (Version 1.4.2; [8]). The T1-weighted (T1w) image was corrected for intensity non-uniformity (INU) with N4BiasFieldCorrection [10], distributed with ANTs 2.2.0 [11], and used as T1w-reference throughout the workflow. The T1w-reference was then skull-stripped with a Nipype implementation of the ANTs brain extraction workflow, using OASIS30ANTs as the target template. Brain tissue segmentation of cerebrospinal fluid (CSF), white matter (WM) and gray matter (GM) was performed on the brain-extracted T1w using fast (FSL, Version 5.0.9; [12]). Brain surfaces were reconstructed using recon-all (FreeSurfer, Version 6.0.1; [13]), and the brain mask estimated previously was refined with a custom variation of the method to reconcile ANTs-derived and FreeSurfer-derived segmentations of the cortical gray matter of Mindboggle [14]. Volume-based spatial normalization to one standard space (MNI152NLin2009cAsym; [15]) was performed through nonlinear registration with antsRegistration (ANTs, Version 2.2.0), using brain-extracted versions of both the T1w reference and the T1w template.

We used subnetwork definitions from previous work [16] which found data-driven parcellations of intrinsic functional connectivity consistent with previously identified regions comprising putative frontoparietal control [17] and dorsal and ventral attention [18] networks. We used a more recent parcellation atlas [4] that remained consistent with these network divisions. The "frontoparietal control network" included regions within the parietal, temporal, orbitofrontal, lateral prefrontal, lateral ventral prefrontal, cingulate, and medial posterior prefrontal cortices and the precuneus. The "dorsal attention network" included regions within

frontal eye fields and the precentral and postcentral gyri. The "ventral attention network" included regions within the insula, parietal operculum, frontal operculum, and the temporal occipital, lateral prefrontal, parietal medial, frontal medial, temporal occipital, temporal parietal cortices, and the precentral gyrus. The standardized spatial coordinates of regions included in each subnetwork are (publicly available).

1.6 Resting-state and task-fMRI data preprocessing

For each of the resting-state and task BOLD scans, the following preprocessing was performed. First, a reference volume and its skull-stripped version were generated using a custom methodology of fMRIPrep. A $B0$-nonuniformity map (or fieldmap) was estimated based on two echo-planar imaging (EPI) references with opposing phase-encoding directions, with 3dQwarp in AFNI [19]. Based on the estimated susceptibility distortion, a corrected EPI reference was calculated for a more accurate co-registration with the anatomical reference. The BOLD reference was then co-registered to the T1w reference using bbregister from FreeSurfer, which implements boundary-based registration [20]. Co-registration was configured with six degrees of freedom. Head-motion parameters with respect to the BOLD reference (transformation matrices, and six corresponding rotation and translation parameters) are estimated before any spatiotemporal filtering using mcflirt (FSL, Version 5.0.9; [21]). BOLD runs were slice-time corrected using 3dTshift from AFNI. The BOLD time-series were resampled onto their original, native space by applying a single, composite transform to correct for head motion and susceptibility distortions. The BOLD time-series were resampled into standard space, generating a preprocessed BOLD run in MNI152NLin2009cAsym space. All resamplings were performed with a single interpolation step by composing all the pertinent transformations (i.e. head-motion transform matrices, susceptibility distortion correction when available, and co-registrations to anatomical and output spaces). Gridded (volumetric) resamplings were performed using antsApplyTransforms (ANTs), configured with Lanczos interpolation to minimize the smoothing effects of other kernels. Non-gridded (surface) resamplings were performed using mri_vol2surf (FreeSurfer). Various confounds (e.g., framewise displacement, DVARS, global signal) were also calculated for each TR. The outputs from fMRIPrep were then manually quality checked to ensure adequate preprocessing.

1.7 fMRI motion regression

Following preprocessing with fMRIPrep, these data were denoised using the xcpEngine pipeline [22]. Specifically, xcpEngine was used to remove motion-related confounds from BOLD sequences using the most stringent of current standards [22]. These steps were as follows: (1) demeaning and removal of linear and quadratic trends from time series, (2) de-spiking using AFNI's 3DDESPIKE utility, (3) temporal bandpass filtering using a first-order Butterworth filter to retain signal in the range 0.01–0.08Hz, (4) 36-parameter confound regression including 6 realignment parameters, mean signal in white matter, CSF and mean global signal, as well as the first power and quadratic expansions of their temporal derivatives. These denoised time series were then used in further analyses. We used Nipype (Version 1.4.2; [8]) and Nilearn (Version 0.7.0; [23]) to extract activity time courses during the mindful attention task. A low-pass filter of 0.1 Hz and a high-pass filter of 0.01 Hz was applied. We added 6 seconds to every event onset to account for hemodynamic delay. For example, if an event took place during 10 to 16 TRs, a time-series was extracted for 16 to 22 TRs. We did not include events shorter than 1 TR (i.e., 1 sec), which were usually fixation periods.

Prior to first-level modeling, we generated motion regressors using an automated motion assessment tool ([24]; https://github.com/dcosme/auto-motion-fmriprep). This tool is a predictive model that utilizes the confound files generated by fMRIPrep and classifies whether or not fMRI volumes contain motion artifacts. The classifier is applied to each participant's task run and returns a binary classification indicating the presence or absence of motion artifacts for each volume. In addition, this tool transforms the realignment parameters into Euclidean distance for translation and rotation separately, and calculates the displacement derivative of each. This procedure yields a total of 5 motion regressors for first-level modeling. Task runs that contain >10% of volumes classified as containing a motion artifact will be excluded from further analyses ($n = 1$). For group-level analyses, multiple comparisons will be corrected using cluster-extent thresholding

was implemented using AFNI [19]. In accordance with recent guidelines [25], the spatial autocorrelation function was first estimated for each subject and task run separately using AFNI's 3dFWHMx on the residuals, and then averaged across subjects. To determine probability estimates of false-positive clusters given a random field of noise, Monte-Carlo simulations were conducted with AFNI's 3dClustSim using the average autocorrelation across subjects. Following motion exclusions, the sample included $n = 37$ mindful and $n = 39$ baseline participants.

1.8 Diffusion data preprocessing

MP-PCA denoising as implemented in MRtrix3's dwidenoise [26] was applied with a 5-voxel window. After MP-PCA, Gibbs unringing was performed using MRtrix3's mrdegibbs [27]. Following unringing, B1 field inhomogeneity was corrected using dwibiascorrect from MRtrix3 with the N4 algorithm [10]. After B1 bias correction, the mean intensity of the DWI series was adjusted so that the mean intensity of the $b = 0$ images was matched across DWI scanning sequences. FSL (Version 6.0.3:b862cdd5)'s eddy was used for head motion correction and eddy current correction [28]. Eddy was configured with a q-space smoothing factor of 10, a total of 5 iterations, and 1000 voxels used to estimate hyperparameters. A linear first level model and a linear second level model were used to characterize spatial distortions related to eddy currents. The q-space coordinates were forcefully assigned to shells. The field offset was attempted to be separated from subject movement. Shells were aligned after eddy current correction. Eddy's outlier replacement was run [28]. Data were grouped by slice, only including values from slices determined to contain at least 250 intracerebral voxels. Groups deviating by more than 4 standard deviations from the prediction had their data replaced with imputed values. Fieldmaps were collected with reversed phase-encode blips, resulting in pairs of images with distortions going in opposite directions. Here, a $b = 0$ fieldmap image with reversed phase encoding direction was used along with $b = 0$ images extracted from the DWI scans. From these pairs, the susceptibility-induced off-resonance field was estimated using a method similar to that described in Ref. [29]. The fieldmaps were ultimately incorporated into the eddy current and head motion correction interpolation. Final interpolation was performed using the jac method.

Several confounding time-series were calculated based on the preprocessed DWI. Framewise displacement (FD) was calculated using the implementation in Nipype (following the definitions in [30]). The head-motion estimates calculated in the correction step were also placed within the corresponding confounds file. Slicewise cross correlation was also calculated. The DWI time-series were resampled to ACPC, generating a preprocessed DWI run in ACPC space with 1.7 mm isotropic voxels. Many internal operations of QSIPrep use Nilearn (Version 0.7.0; [23]) and Dipy [31].

1.9 Ecological assessment measure of drinking

Drinking was defined as the number of alcohol servings consumed per assessment distributed throughout the 28-day period. To obtain the number of alcohol servings per occasion, we summed the number of wine, beer, and liquor drinks at each signal level. The three largest and improbable values of drinks per drinking occasion (24, 36, 60) observed across three individuals, were set to 16 drinks per occasion. We observed no substantial differences in results when including these outlier values in the main models as part of additional sensitivity analyses.

1.10 Task stimuli

Stimuli were presented using PsychoPy [32] and participants responded to stimuli using a five-button box. The reliability of the alcohol cues were established in a prior study [33]. In this prior study, researchers studied how the emotional valence of alcohol cues related to different levels of drinking behavior. College students were stratified into three groups (non-drinkers, low risk drinkers, and high risk drinkers) by a well-validated assessment [34]. All participants rated the emotional valence (pleasure/displeasure) and arousal (excitement/calm) of stimuli on 9-point scales [35]. High risk drinkers exhibited greater valence scores for

alcohol images than non-drinkers and low risk drinkers. All participants exhibited greater arousal for alcohol images than non-alcohol images. The images had high internal consistency of self-reported valence and arousal within the drinking groups.

Additionally, the image set was normed and tested for subjective (complexity) and objective (brightness and color) values. The images did not include beverage brands to avoid confounds with brand preference and balanced the social contexts of the cues. Finally, participants were able to reliably recognize the type of beverage ($> 95\%$).

1.11 Operationalizing mindful attention

Mindful attention is thought to support psychological distancing by decentering one's cognitive and emotional experience [36]. This operationalization of mindful attention has been linked to down-regulating negative affect, pain, and nicotine craving [37, 38, 39]. Notably, these studies demonstrate that mindful attention can be an effective self-regulatory strategy for people with no experience in meditation. As a self-regulatory strategy, a mindful attention task can help elicit psychological distancing and reduce craving, representing a practical short-term preventative approach in contrast to longer-term formal interventions.

Our operationalization of mindful attention parallels the open monitoring component of mindfulness [40, 41]. Open monitoring involves psychological distance, non-reactive meta-cognitive monitoring, and non-reactive awareness of automatic cognitive and emotional interpretations of exogenous and endogenous stimuli [40, 41]. When people practice mindfulness with an emphasis on open monitoring, they might quickly and less emotionally become aware of their sense of identity based on past memories and expected future experiences [40]. Prior hypotheses state that brain regions involved in open monitoring may also be implicated in vigilance and disengaging attention from information that distracts one from the present, ongoing stream of experience. Consistent with these hypotheses, we found that mindful attention elicited a present-focused flow of neural dynamics of the frontoparietal, dorsal attention, and ventral attention networks. Frontoparietal regions have been previously associated with the engagement and disengagement of attention, while dorsal and ventral attention regions have been associated with vigilance to salient information [42, 18]. Present-focused neural dynamics involve effortful control input in addition to a reduced propensity to dwell on neural states. Our model suggests that training can increase the efficiency of mechanisms that non-linearly lower the effortful control input required to engage or disengage from the ongoing stream of experience.

The baseline (natural react) trials are different from traditional meditative practices like Vipassana because baseline trials. This difference arises from the instructions allowing natural reactions to include judgment, elaborated cognitive and emotional processing, and lack interoception—all in contrast to Vipassana. Vipassana, in turn, is more similar to our mindful attention condition due to a shared focus on psychological distance and non-judgmental, meta-cognitive awareness. We used natural reactivity as the experimental control because it contrasts of mindfulness characterized by open monitoring, non-reactive meta-cognitive monitoring, and non-reactive awareness of cognitive and emotional interpretations of exogenous and endogenous stimuli, and reduced evaluation and judgement that amplify the initial event. Operationalizing mindful attention thus opposes the *natural reactivity* of gut reactions, which may include judgment, include elaborated cognitive and emotional processing, and lack interoception. Notably the instructions for mindful attention include explicit directions to observe the situation without judgement, and these instructions are also common to mindfulness inductions as traditionally used in meditative practices like Vipassana, which necessarily include interoception and non-judgmental awareness. To better elucidate different types of attention that occur during experimental conditions, future work could use machine learning classifiers to identify the modes of attention that are elicited by different mindfulness instructions [43]. This research could also elucidate the extent the mindful attention instructions or react naturally baseline constituted a placebo because placebo effects tend to focus on spatially separable brain systems [44, 45].

1.12 Task Instructions and Piloting

As reported previously in Jovanova *et al.* [46], researchers guided participants through the instructions on how to respond to alcohol cues on a computer screen in a laboratory setting. During practice, participants completed an abbreviated version of the fMRI task in which they viewed image cues of alcoholic and non-alcoholic beverages while being prompted to react naturally or to respond with mindful attention. Researchers verbally checked participant comprehension. This procedure was replicated in a separate sample collected remotely during the COVID-19 pandemic [46]. The instructions used to operationalize mindful attention focused on maximizing the self-distancing and de-reification aspects of mindfulness [47, 48, 49, 50]. We developed instructions to train the short-term induction of mindful attention following prior work that demonstrated the efficacy of short-term training [38, 37]. We allocated 30 minutes for training. The training session begins with the message:

> Now we'll practice the second task that you'll complete in the scanner. This task will feel very long in the scanner - it will take 30 minutes. This is because we need a lot of examples of how your brain responds. Try to stay focused even if it feels repetitive.

The full instructions for the short-term induction of mindful attention in response to alcohol cues were:

> Another way you can relate to these situations is by mentally taking a step back in order to observe the situation and your response to it in an impartial and nonjudgmental manner.
>
> You may simply notice your thoughts and feelings about these situations, perhaps with some curiosity. That way, you can actively pay attention to your reaction and see it as just a passing pattern of thoughts and feelings, without getting caught up in it.
>
> If you see a picture of beer, you can mentally distance yourself by observing the situation, and your response to it, with a more impartial, nonjudgmental, or curious mindset. When you see the word MINDFUL, it is critical that you mentally take a step back from the situation, so that you observe the situation and your response to it without getting caught up in it.

The training involved 8 trials of viewing stimuli that lasted 6 seconds each on the screen, followed by a fixation cross and a prompt asking for the craving rating (see also **Figure 1A** of the main text). To inform the language of the mindful attention intervention, we explored nine different variations of mindfulness-related instructions [46]. Following the report of [46] on the same data, we describe here a series of 14 online studies via Amazon's Mechanical Turk (total $n = 700$) to test manipulation effects on craving evoked by viewing alcohol cues. In each pilot, participants viewed one of 9 different versions of mindfulness instructions on some trials and control instructions on other trials. Three of the pilots emphasized instructions related to psychological distancing, whereas the remaining versions emphasized different components, such as attention to the present moment, focus, awareness, or acceptance, and contained no distancing language. We chose the instructions described in the main text that focused on psychological distancing because they tended to decrease alcohol craving ratings more than did other types of instructions.

We used methods described in detail in a separate publication [46]. Briefly, participants were probed with EMA surveys twice a day for 28 days for a total of 56 surveys. EMA surveys were sent via LifeData (https://www.lifedatacorp.com/), an EMA application installed on participants' smartphones. Participants also received two prompts daily on how to respond to alcohol cues in daily life twice a day for 28 days for at total of 56 signals. We observed high compliance with a median response rate of $91\%(50.97 \pm 7.13)$.

For the survey, we measured drinking behavior with several questions sent at 8:00 am and 6:00 pm. To assess drinking behavior, a question stated, "Since your EVENING/MORNING survey, have you consumed

any alcohol? ("No" or "Yes" response option)." Participants who responded "Yes", were asked to enter the number of standard servings of beer, liquor, and wine consumed since the previous survey using numeric entry. When participants responded "No" to having consumed alcohol, they answered questions about physical activity, caffeine use, and water consumption. These questions were matched for length with the follow-up alcohol questions to minimize the possibility that participants would report no alcohol use in order to minimize survey completion time. The survey also included questions about mood, conversations about alcohol, and others that were not the focus of our paper.

In the text reminder prompts, we sent a message to baseline participants at 2:00 pm and 9:00 pm each day that stated "If you are around alcohol today, REACT NATURALLY—have whatever thoughts and feelings you would normally have". We sent a message to the mindful attention participants that stated "If you are around alcohol today, REACT MINDFULLY—notice, acknowledge, and accept the thoughts and feelings you have." For descriptive statistics on the demographics of our participants, study enrollment and retention, and replication in a separate sample, please see Ref. [46].

1.13 Manipulation checks

After the scan session, participants answered survey questions about the cognitive strategies that they used during the task and their level of confidence using the strategies. When participants in the mindfulness condition endorsed encountering alcohol during the morning and evening surveys of the EMA protocol, two follow-up questions acted as manipulation checks: "Since the Morning/Evening survey, I reacted naturally to alcohol" and "Since the Morning/Evening survey, I reacted mindfully to alcohol". Participants responded to these questions on a scale from 1 ("Strongly Disagree") to 100 ("Strongly Agree"). To capture practice over the entire 4 weeks of the EMA protocol, participants also responded to the following question in the last survey of the EMA protocol: "When you encountered/were around alcohol during the past 4 weeks (i.e., since you started getting surveys on your phone), how often did you REACT NATURALLY to alcohol?" and "When you encountered/were around alcohol during the past 4 weeks (i.e., since you started getting surveys on your phone), how often did you REACT MINDFULLY to alcohol?" Participants responded to these questions on a scale from 1 ("Never") to 100 ("All the time"). See Supplementary Results and Figure 6 for evidence supporting manipulation effects.

1.14 Statistical modeling

To examine associations between mindful attention and average controllability on drinking throughout the 28-day EMA protocol, we used multilevel models. The multilevel models accommodated the nested nature of the smartphone sampling data including 56 total alcohol conversation signals and 56 total drinking signals, nested in 104 participants across 10 social groups. We chose a multilevel hurdle model [51] using glmmTMB in R, specifying a truncated negative binomial function [52]. Count data such as alcohol use data in the present case (i.e., number of drinks consumed) are often positively skewed and include many observations at zero. Hurdle models are often used to model this type of data as these include both a count regression (in this case Poisson/negative binomial) to model the counts, and a logistic regression to model the zeroes in the data. Here, all the counts are modeled by a truncated Poisson/negative binomial (i.e., truncated as it does not contain zero), and all the zeroes (non-alcohol use occasions) are modeled with the logistic regression. Thus, using these models allowed us to independently model and isolate how much a person drinks when they drink, our primary outcome, and to model the probability of whether a person drinks or not at a given occasion as part of secondary analyses. We specified nested random effects to include participant ID and group ID, given that the repeated conversational valence and drinking observations are nested within participants over 28 days, and those participants in turn are nested within 10 social groups.

Recent work used the most parsimonious models of alcohol consumption behavior change by controlling for a number of covariates described below (manuscript in preparation). First, to isolate occasions when participants talked more positively about alcohol, relative to their own baseline and prior to a drinking occasion

at the within-person level, we controlled for each person's usual month level between-person alcohol conversation valence over the 28 days. We additionally controlled for time in the study, as individuals reported drinking less towards the end of the ecological momentary assessment period; social weekend (Thursday, Friday, or Saturday vs. weekday), given different drinking patterns on "college weekends" vs. weekdays among students [53]; and smartphone survey response rates. We additionally controlled for demographic variables such as gender, as drinking patterns often vary across gender [54]; age, the number of alcohol conversations, and randomization into a drinking intervention as part of a different study. Sensitivity analyses were conducted to test for the robustness and overfitting of subsets of these models (manuscript in preparation).

In this work, we were additionally interested in assessing how average controllability influences later drinking. Following prior work studying the effects of loving-kindness meditation and self-affirmation on self-regulation and behavior change [55], we controlled for additional covariates of baseline drinking, race/ethnicity, and years of education. Including baseline measurements for the frequency or amount of drinking alters the primary outcome model to be the residualized change from drinking at baseline to drinking during the mindful attention training [56]. Despite the usefulness of the baseline-adjusted outcome variable, it can ultimately bias estimates [57]. Therefore, we conducted a sensitivity analysis without the baseline and found consistent results with or without this covariate as well as the next demographic and personality trait covariates that we describe (**Supplementary Figure 2**).

Demographic covariates are useful to model individual differences in education, gender, and race/ethnicity that are known from prior research to be implicated in alcohol use [58] and meditation training [59, 60]. Lower levels of education have been associated with more consumption of alcohol [61]. In the context of our study, we included the years of education to account for the observation that undergraduates consume alcohol differently over the course of their time in college, for example consuming more alcohol during their first year than in later years [62]. Prior research has also reported racial/ethnic differences in rates of alcohol consumption [63], which can be partially explained by several factors including individual differences in alcohol-related beliefs and contextual influence from cultural orientations to alcohol consumption [64].

Lastly, we controlled for the personality trait of attentional impulsivity for four reasons. First, prior work suggests that self-reported mindfulness is negatively correlated with self-reported impulsivity [65]. Second, prior work suggests that controlling for baseline personality differences could strengthen analytic designs that test for the effects of mindfulness [66]. Third, despite differences in and debate regarding the definition of mindfulness as used by practioners, clinicians, and psychologists, the regulation of attention is a shared component [41]. Fourth and finally, mindfulness meditation has been shown to facilitate attention regulation *and* emotion regulation, supported by a relationship between self-reported levels of mindfulness and self-reported measures of adaptive emotion regulation strategies, even after controlling for symptoms of stress, anxiety, and depression [67]. Attention impulsivity was positively correlated with difficulties in emotion regulation in our dataset and was not collinear with average controllability (**Supplementary Figure 1**).

The final models are the zero-inflated model of logistic drinking probability as a binary outcome and the conditional model of the count of drinking amount. They can be written as

$$\text{Drinking probability} \sim b_0 + b_1(\text{Condition}) + b_2(\text{Time}) + b_3(\text{Gender}) + b_4(\text{Number of responses}) + b_5(\text{Social Weekend}) + b_6(\text{Baseline drinking frequency}) + b_7(\text{Age}) + b_8(\text{Intervention week}) + b_9(\text{Average controllability}) + b_{10}(\text{Race/ethnicity}) + b_{11}(\text{Years of education}) + b_{12}(\text{Attentional impulsivity}) + (1|\text{group/participant}).$$

$$\text{Drinking amount} \sim b_0 + b_1(\text{Condition}) + b_2(\text{Time}) + b_3(\text{Gender}) + b_4(\text{Number of responses}) + b_5(\text{Social Weekend}) + b_6(\text{Baseline drinking amount}) + b_7(\text{Age}) + b_8(\text{Intervention week}) + b_9(\text{Average controllability}) + b_{10}(\text{Race/ethnicity}) + b_{11}(\text{Years of education}) + b_{12}(\text{Attentional impulsivity}) + (1|\text{group/participant}).$$

The predicted probability of drinking was plotted by using the regression model to generate predicted values of the marginal effect of average controllability.

1.15 Network Control Theory

Average controllability
From the DWI data, we constructed anatomical brain networks by subdividing the brain into 414 regions using the Schaefer atlas for 400 cortical regions and the Harvard Oxford atlas for 14 subcortical regions [4, 5, 68]. In these anatomical connectivity matrices, brain regions are defined as nodes, and a link between two nodes represents the number of streamlines connecting them. Controllability of a dynamical system describes the possibility of driving the current state of a system to a desired target state via external control input [69]. Such an approach allows us to gain better insight into the relationship between brain structure and brain dynamics. Here, we focus on average controllability, which quantifies each region's capacity to leverage the brain's underlying structural connectivity to distribute activity throughout the brain to guide changes to any new hypothetical states [70]. Networks with high average controllability are more influential in the control of network dynamics than networks with low average controllability. The relationship between the mathematical formulation of network control and brain networks is discussed in more detail elsewhere [71].

To ensure system stability, each participant's structural connectivity matrix was normalized by dividing each element by the largest absolute eigenvalue of the matrix plus one [69]. Following normalization, average controllability was calculated for each node. Finally, we calculated the mean average controllability over nodes. These person-averaged estimates of average controllability were then considered further in the subsequent analyses of between-person differences.

Optimal control inputs. We begin by approximating brain state dynamics through the linear continuous-time equation

$$\dot{x}(t) = Ax(t) + Bu(t), \tag{1}$$

where, for the task fMRI data, $x(t)$ is a vector of size $N \times 1$ (where N is the 414 brain regions in the network, consisting of 400 cortical regions and 14 subcortical regions) that represents the state of the system at time t, A is the weighted symmetric $N \times N$ structural matrix estimated through diffusion spectrum imaging, B is an input matrix of size $N \times N$ specifying the set of control nodes, and $u(t)$ is the time-dependent control signal in each of the control nodes. When analyzing the resting-state fMRI data, $x(t)$ is defined as a N x 1 vector from the the N x R BOLD time series, where R is the set of 300 images acquired at each repetition time during the scan. The optimal control energy framework [69] defines the unique control input $u^*(t)$ needed to transition the system from an initial state $x(0) = x_0$ to a final target state $x(T) = x_T$ over the time horizon T through the cost function that solves the problem:

$$\begin{aligned} \boldsymbol{u}(t)^*_\kappa &= \underset{u_K}{\operatorname{argmin}} J\left(\boldsymbol{u}_\kappa\right) = \underset{\boldsymbol{u}_\kappa}{\operatorname{argmin}} \int_0^T \\ &\left(\left(\boldsymbol{x}_T - \boldsymbol{x}(t)\right)^\top \left(\boldsymbol{x}_T - \boldsymbol{x}(t)\right) + \rho \boldsymbol{u}_\kappa(t)^\top \boldsymbol{u}_\kappa(t)\right) dt, \end{aligned} \tag{2}$$

where the parameter ρ determines the relative weighting between the costs associated with the length of the state trajectory and the input energy. Following prior work, we set δ to 1 such that no specific assumptions are made about the relative importance of constraints on energy and distance values [69]. The cost function $J(\boldsymbol{u}(t)^*_\kappa)$ is defined to find the unique optimal control input $\boldsymbol{u}(t)^*_\kappa$. We then use this optimal control input to calculate the control inputs required by a single brain region:

$$E_i^* = \int_0^T \|u_i^*(t)\|_2^2 \, dt. \tag{3}$$

By integrating each control input over time, we can calculate the total control energy required by all brain regions:

$$E^* = \int_0^T u(t)^{\mathrm{T}} u(t) dt. \tag{4}$$

In order to model the unique importance of the 145 regions of the dorsal attention, ventral attention, and frontoparietal networks, we continued to assign these regions a value of $B = 1$ (as in the previous simulations) and set all other regions as $B = 0.75$. This choice follows prior modeling decisions utilizing a full control set [72, 73, 74]. Finally, we simulated network dynamics while incrementally decreasing the value of B for the 20 precuneus/PCC regions using $B = [0.75, 0.50, 0.25, 0.10, 0.05]$. Following prior work showing that the choice of T results in high correlated (Pearson's $r > 0.99$) control input values across different values of T, we chose $T = 3$ [75].

The persistence energy is the control input E_i^* required to transition from x_T to x_T. With the terminology above, persistence energy defines $x_0 = x_T$. Assuming that states which require greater persistence energy are less stable, the control stability S of a neural state is defined as

$$S = \frac{1}{\log_{10}\left(E_{x_0 = x_T}\right)}. \tag{5}$$

2 Supplementary Results

2.1 Network control theory

Network control theory provides a suite of tools to interrogate the effort of network dynamics during mindful practice. There exist strong interrelationships among the different control metrics of average controllability, optimal control input, and control stability. By averaging these metrics across all participants to obtain mean regional values, we observed that brain regions with greater average controllability can efficiently reach any hypothetical state and tend to be the optimal regions to receive more control input (Spearman's $\rho(142)$=0.59, p<0.001). These regions with greater average controllability tend to have reduced control stability ($\rho(142)$=-0.59, p<0.001), suggesting that the regions favor different rather than stably persisting states. The strong interrelationships among the control metrics suggest that while each metric offers a distinct interpretation of brain function that is helpful for a fuller understanding of the neural dynamics of mindfulness, they may collectively contribute to regulatory processing.

2.2 Multi-level model of drinking behavior and sensitivity analysis

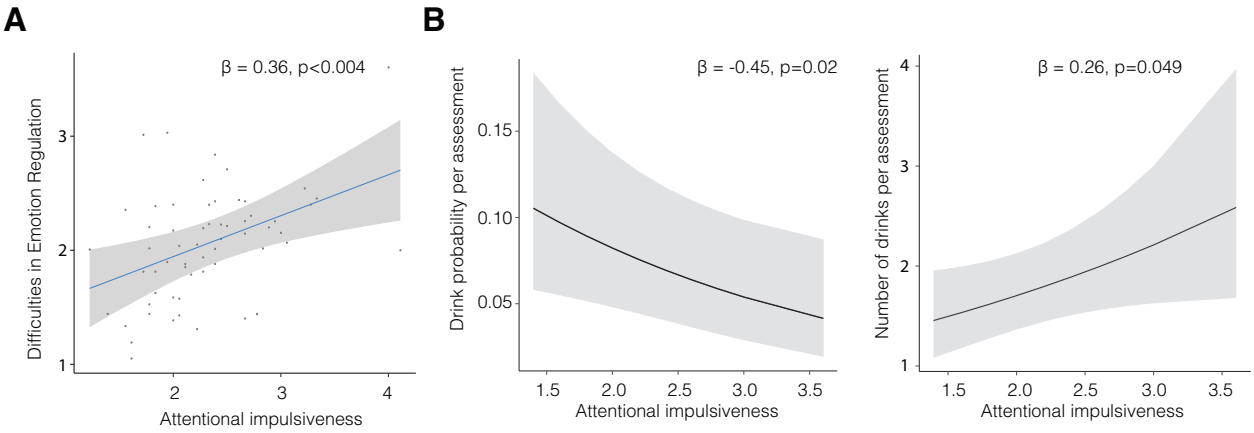

Figure 1: **(A)** Participants who have greater self-reported attentional impulsiveness also have greater self-reported difficulties in emotion regulation. **(B)** The multi-level model reported in the main results also indicated that participants who had greater attentional impulsiveness were less likely to drink, but they drank more if they did drink.

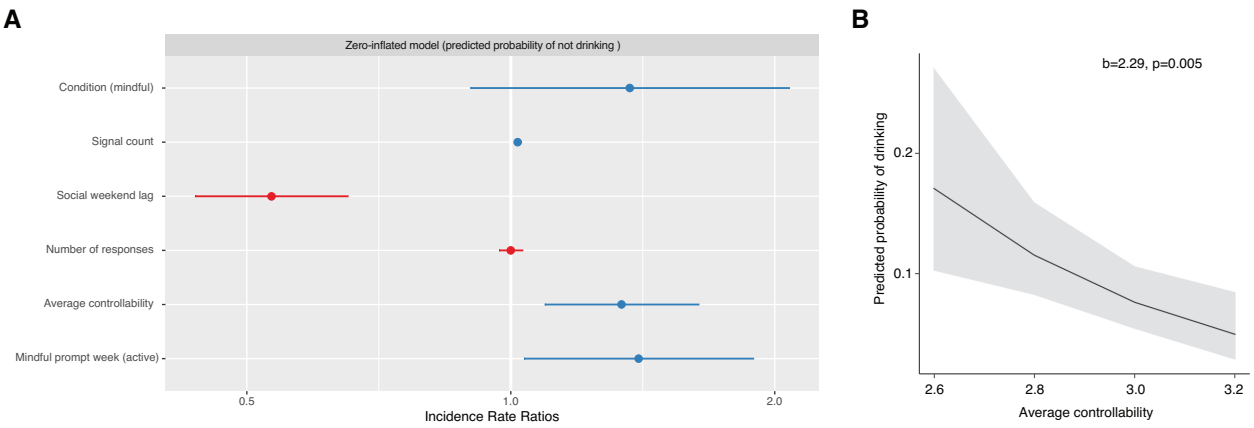

Figure 2: **Sensitivity analysis for average controllability predicting later behavior change in the moderation of alcohol consumption. (A)** A sensitivity analysis showing the results of the most parsimonious model. **(B)** We observed consistent findings with and without additional covariates of baseline drinking amount or frequency in the past 6 months, demographic variables, and the personality trait of attentional impulsivity. As reported in [46], when participants received text reminders to respond mindfully to alcohol cues that they encountered in their daily lives, participants reduced their drinking frequency from once every 6 days to once every 8 days.

2.3 Exploratory analysis of regional differences in task-related activation

A

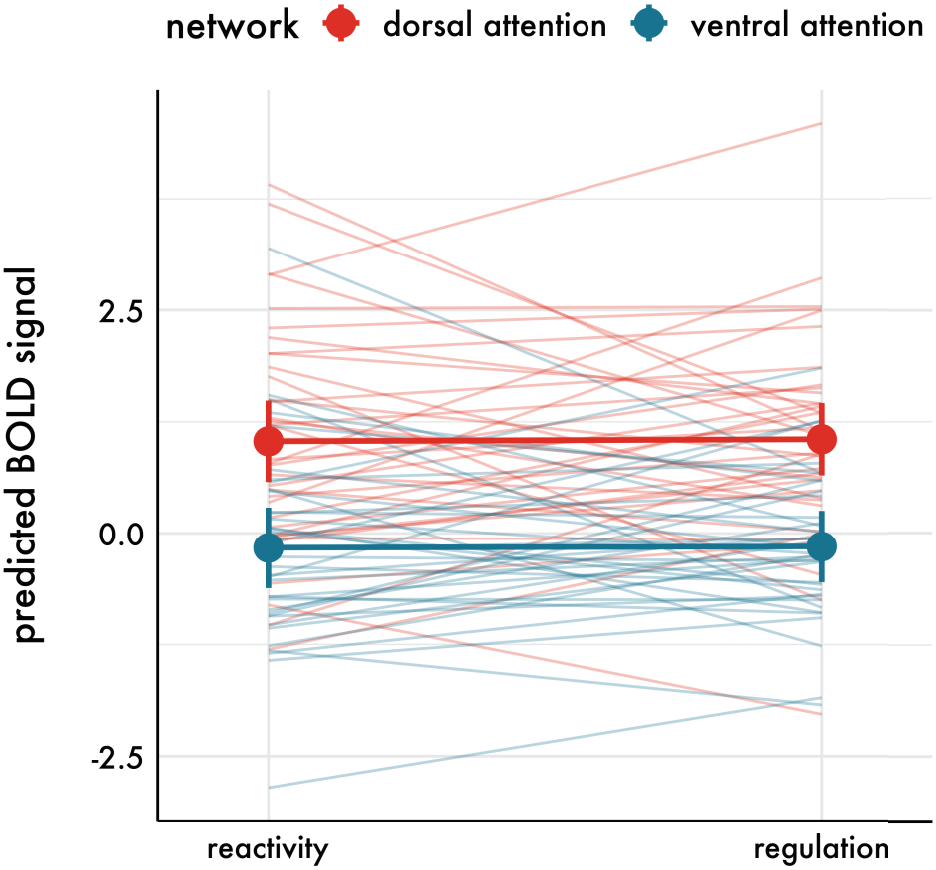

B

Variable	Estimate	Standard error	df	t-value	p-value
Intercept	1.03	0.23	79.02	4.44	0.000029
Trial condition (mindfully attend to alcohol)	0.0	0.18	37.60	0.13	0.90
Type of network (ventral attention)	-1.20	0.20	94.34	-6.0	0.000000036
Trial condition-by-network interaction	-0.008	0.05	6715.0	-0.15	0.88

Figure 3: **No differences in network activation between conditions. (A)** We used a linear mixed model fit by restricted maximum likelihood, modeling random effects for the participant, brain region, and trial type. We assessed main effects of the trial condition, network, and the trial-by-network interaction. We did not find differences in neural activity between conditions at the network level ($b = 0.02$, $p = 0.90$) nor an interaction ($b = -0.01, p = .878$). **(B)** A summary table of the model results.

We did not find differences in the average neural response at the whole-brain level between groups or conditions (whole-brain contrast maps are publicly available here [76]). This result does not preclude the possibility that regional differences exist. Future work using *a priori* masks to study regional activation will be important. For example, in separate work using this dataset, it was recently reported that feelings of purpose in life influenced whether greater alcohol cue reactivity within the ventral striatum was associated with increased or decreased alcohol use following craving in daily life [77]. Based on prior work, the ventral

striatum was an *a priori* region of interest [78, 79].

We also conducted an exploratory analysis of average differences in regions broadly associated with attention (**Supplementary Figure 3**; **Table 1**) [16]. We found that the most activated regions included the bilateral precuneus, left middle temporal gyrus, left insula, and bilateral superior parietal cortices. These regions have been associated with imagery, action observation, temporal processing, theory of mind, empathy, pain, somatosensation, and working memory [80]. The most deactivated regions included the right precuneus, right inferior parietal cortex, left precentral gyrus, opercular part of inferior frontal gyrus, and the right supramarginal gyrus. These regions have been associated with somatosensation, working memory, language, imagery, consciousness, error, and expectancy [80].

We also wish to highlight the different assumptions made by an analysis of regional activity and of a dynamical systems model. In an analysis of regional activity, if one does not find statistically significant differences in the regional neural activity elicited by the task, then one typically assumes that those regions are not implicated in the brain function. In contrast, a dynamical systems model assumes that regional activity contributes to a task-elicited dynamical trajectory. This trajectory may be largely driven by the activity of a subset of regions. However, in network control theory, the contribution of regional activity also depends on how regional activity flows along the anatomical white matter connections. Indeed, the probability of a neural state is related to the control input needed to drive it as well as the controllability admitted by anatomical white matter pathways that connect regions [81]. Our main findings support the sensitivity of the network control theory framework to investigate task-related changes at the network level which may be obscured by average differences in activity magnitude.

Name (Schaefer atlas)	**Name (AAL)**	**X**	**Y**	**Z**	**BOLD**	**Neurosynth key word association**
Left Med_7	Supp_Motor_Area_L	-8	-2	70	0.34	execution, motor, imagery, production
Left Post_15	Precuneus_L	-8	-58	64	0.33	tracking, imagery, action observation, expertise
Left FEF_1	Precentral_L	-40	-2	52	0.33	premotor, movements, eye, finger
Left Post_3	Temporal_Mid_L	-56	-62	0	0.31	temporal, objects, tools, lexical
Left Post_4	Temporal_Mid_L	-48	-66	16	0.3	action observation, theory of mind, intentions, empathy
Right Med_5	Precuneus_R	10	-44	54	0.29	body, abilities, abstract, accuracy
Left FrOperIns_4	Insula_L	-40	-14	-2	0.28	pain, somatosensory, noxious, autobiographical
Left Post_7	Parietal_Sup_L	-22	-66	46	0.26	working memory, task, load, demands
Left Post_16	Parietal_Sup_L	-20	-56	66	0.26	movements, pointing, action observation, imagery
Right Post_12	Parietal_Sup_R	20	-68	52	0.26	calculation, saccade, visuospatial, subtraction
Right Post_6	SupraMarginal_R	58	-22	44	-0.34	somatosensory, finger, hand, motor
Right Post_15	Precuneus_R	8	-72	52	-0.34	working memory, memory, calculation, execution
Right Post_8	Parietal_Inf_R	44	-38	50	-0.33	tasks, calculation, spatial, finger
Right Post_11	Parietal_Inf_R	36	-44	44	-0.33	tasks, working memory, premotor, finger movements
Right Post_9	Postcentral_R	46	-28	42	-0.31	finger movements, hand, motor
Left PrCv_1	Precentral_L	-50	6	26	-0.29	phonological, language, reading, working memory
Left Post_8	Parietal_Inf_L	-46	-30	44	-0.25	finger, hand, somatosensory, grasping
Right FrOperIns_8	Frontal_Inf_Oper_R	54	12	12	-0.25	motor, music, execution, imagery
Right TempOccPar_7	SupraMarginal_R	62	-38	36	-0.24	consciousness, motor imagery, error, expectancy
Left Post_6	Parietal_Inf_L	-54	-32	44	-0.23	premotor, finger, grasping, hand, tools

Table 1: **Brain regions with the most relative activation or deactivation in the dorsal and ventral attention networks.** Region names are based on a 400-region parcellation publicly available [4]. We have also included the corresponding automated anatomical labeling (AAL) atlas label [82]. X,Y, and Z coordinates are provided in MNI152 space for region centroids. We list regions with the most activated or deactivated BOLD activity (standardized mean parameter estimates) elicited by mindful attention. Key words associating brain functions from literature to the centroid locations were compiled from the Neurosynth meta-analytic framework [80]. The most activated regions have been associated with imagery, action observation, temporal processing, theory of mind, empathy, pain, somatosensation, and working memory [80]. The most deactivated regions have been associated with somatosensation, working memory, language, imagery, consciousness, error, and expectancy [80].

2.4 Craving during the cue-reactivity task

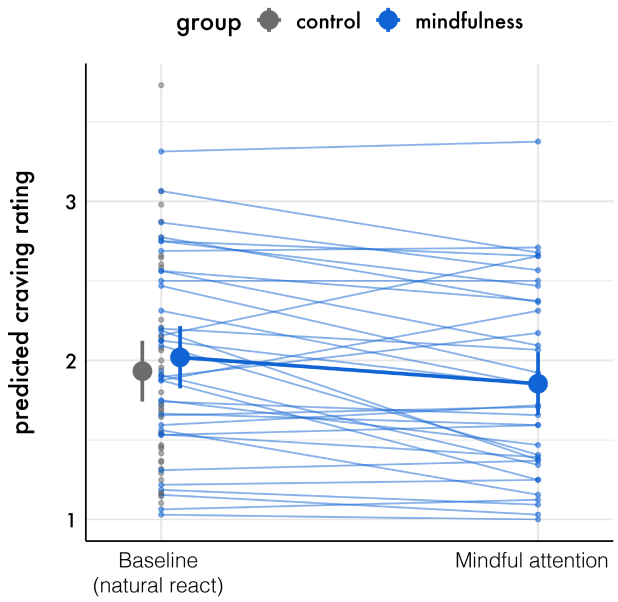

Figure 4: **Regulating with mindful attention reduces craving.** Cues elicited craving as evidenced by reported craving being non-zero in both the baseline and mindful attention conditions ($b = 1.93$, $p < 0.001$). There was no difference in average craving between groups. Within the mindful attention condition, when participants regulated their reactions, they reported less craving than they did when responding naturally in the baseline condition ($b = -0.17$, $p = 0.003$).

2.5 Intrinsic timescales related to the control and stability of task activity

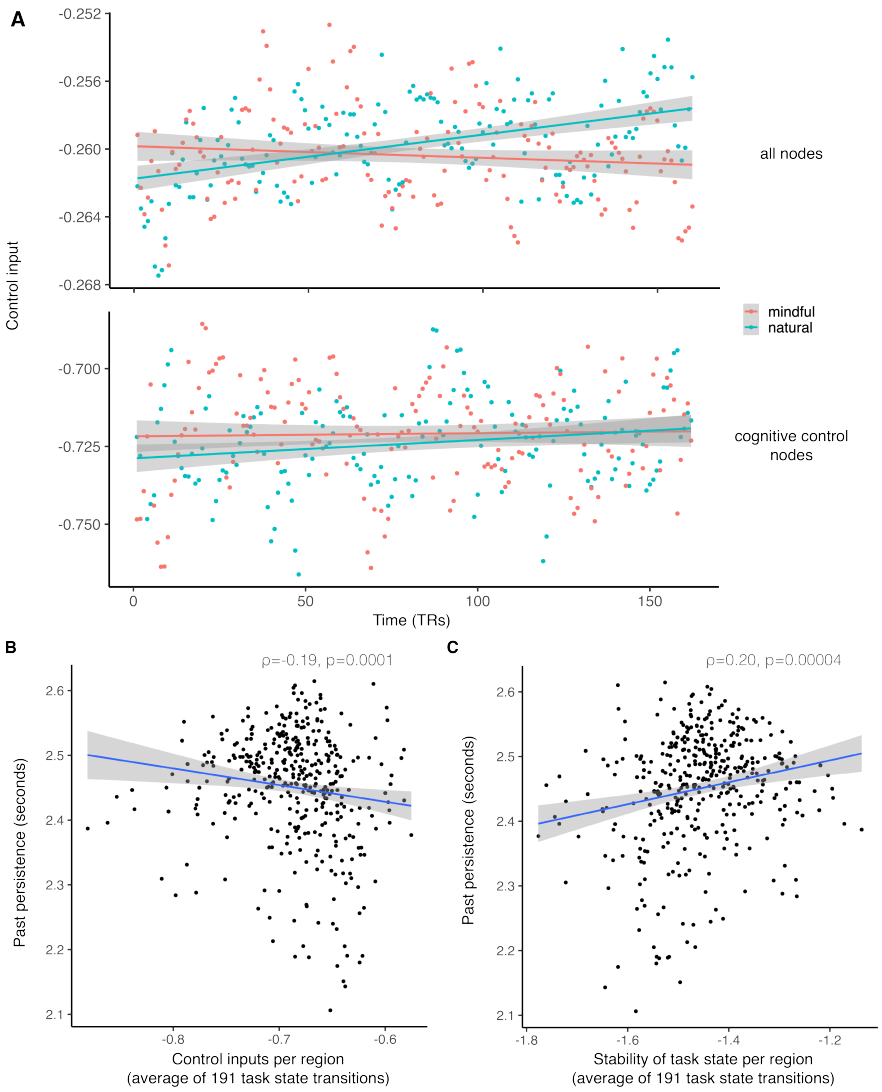

Figure 5: **(A)** Top: For participants in the mindful group, the control input required for naturally reacting was less than that required for mindful attention ($t = -3.3$, $p = 0.001$), suggesting that mindful attention recruits additional effort to de-automatize habitual reactions. The control input required to naturally react tended to increase over time ($\rho = 0.42$, $p < 0.001$), suggestive of more effort and learned de-automatization of habitual reactions. There was an interaction between time and condition ($t = 5.3$, $p < 0.001$), where natural reactions became more effortful while mindful attention became more efficient. Bottom: We found similar results when considering only cognitive control nodes (frontoparietal attention, dorsal attention, and ventral attention). Within subjects, the control input required for naturally reacting was less than that required for mindful attention ($t = -2.1$, $p = 0.04$). The control input required to naturally react tended to increase over time ($\rho = 0.18$, $p = 0.02$). There was no interaction between time and condition. In these simulations, we constructed B such that all nodes could receive control input [74]. The intrinsic neural timescale is a property of ongoing, spontaneous brain activity across the whole brain rather than restricted to only task-responsive regions [83]. **(B)** Intrinsic timescales, which we refer to here as past persistence, describe temporal windows that may be arranged hierarchically such that the computational timescales increase as activity propagates from unimodal sensorimotor to transmodal frontoparietal, default mode, and limbic cortices [84]. Faster timescales correlate with more control input. Slower timescales correlate with more control stability.

A within-person analysis of the manipulations checks (**Supplementary Figure 6**; [**Figure 6** of this Response Document]) indicates that individuals in the mindfulness condition were significantly more likely to respond to alcohol prompts *mindfully* on active weeks when they were prompted to respond mindfully versus on inactive weeks when they were prompted to respond naturally ($B = 18.06$, 95% CI $[13.12, 23.00], p < .001$; active week (mean $= 59.6 \pm 17.7$) vs. inactive week (mean $= 49.5 \pm 21.7$). A between-groups analysis of the manipulation checks suggests practice effects. On average, individuals in the mindful attention condition responded to alcohol prompts *naturally* less frequently relative to individuals in the baseline condition over the 28 days (Welch two-sample t-test $t(40.217) = -6.8, p < 0.001$; baseline condition mean$= 89.6 \pm 10.6$ vs. mindful attention condition mean$= 58.5 \pm 22.2$).

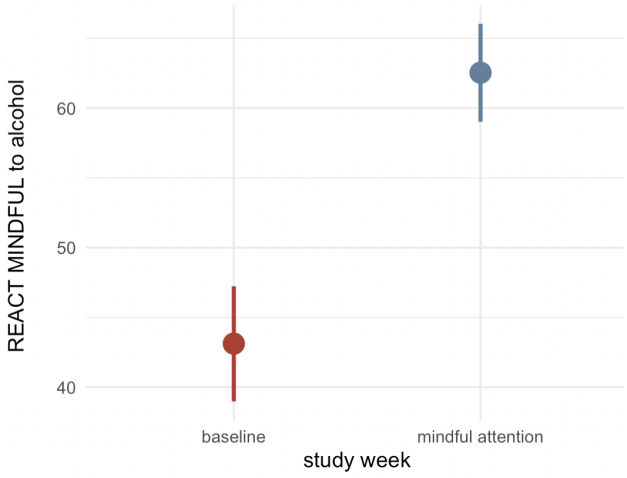

Figure 6: **Manipulation checks for EMA text reminders** Within-person manipulation checks suggest the participants practiced mindful attention in response to EMA reminders.

References

[1] K. J. Gorgolewski, T. Auer, V. D. Calhoun, R. C. Craddock, S. Das, E. P. Duff, G. Flandin, S. S. Ghosh, T. Glatard, Y. O. Halchenko, *et al.*, "The brain imaging data structure, a format for organizing and describing outputs of neuroimaging experiments," *Scientific data*, vol. 3, no. 1, pp. 1–9, 2016.

[2] Y. Halchenko, M. Goncalves, M. V. di Oleggio Castello, S. Ghosh, M. Hanke, M. Brett, T. Salo, C. F. Gorgolewski, J. Stadler, john lee, pvelasco, D. Lurie, J. Pellman, B. Poldrack, B. Schiffler, M. Szczepanik, and J. Carlin, "nipy/heudiconv: Heudiconv v0.5.1," July 2018.

[3] M. Cieslak, P. A. Cook, X. He, F.-C. Yeh, T. Dhollander, A. Adebimpe, G. K. Aguirre, D. S. Bassett, R. F. Betzel, J. Bourque, *et al.*, "Qsiprep: an integrative platform for preprocessing and reconstructing diffusion mri data," *Nature Methods*, pp. 1–4, 2021.

[4] A. Schaefer, R. Kong, E. M. Gordon, T. O. Laumann, X.-N. Zuo, A. J. Holmes, S. B. Eickhoff, and B. T. Yeo, "Local-global parcellation of the human cerebral cortex from intrinsic functional connectivity mri," *Cerebral cortex*, vol. 28, no. 9, pp. 3095–3114, 2018.

[5] S. M. Smith, M. Jenkinson, M. W. Woolrich, C. F. Beckmann, T. E. Behrens, H. Johansen-Berg, P. R. Bannister, M. De Luca, I. Drobnjak, D. E. Flitney, *et al.*, "Advances in functional and structural mr image analysis and implementation as fsl," *Neuroimage*, vol. 23, pp. S208–S219, 2004.

[6] F.-C. Yeh, V. J. Wedeen, and W.-Y. I. Tseng, "Generalized q-sampling imaging," *IEEE transactions on medical imaging*, vol. 29, no. 9, pp. 1626–1635, 2010.

[7] F.-C. Yeh, T. D. Verstynen, Y. Wang, J. C. Fernández-Miranda, and W.-Y. I. Tseng, "Deterministic diffusion fiber tracking improved by quantitative anisotropy," *PloS one*, vol. 8, no. 11, p. e80713, 2013.

[8] K. Gorgolewski, C. D. Burns, C. Madison, D. Clark, Y. O. Halchenko, M. L. Waskom, and S. S. Ghosh, "Nipype: a flexible, lightweight and extensible neuroimaging data processing framework in python," *Frontiers in neuroinformatics*, vol. 5, p. 13, 2011.

[9] O. Esteban, C. J. Markiewicz, R. W. Blair, C. A. Moodie, A. I. Isik, A. Erramuzpe, J. D. Kent, M. Goncalves, E. DuPre, M. Snyder, *et al.*, "fmriprep: a robust preprocessing pipeline for functional mri," *Nature methods*, vol. 16, no. 1, pp. 111–116, 2019.

[10] N. J. Tustison, B. B. Avants, P. A. Cook, Y. Zheng, A. Egan, P. A. Yushkevich, and J. C. Gee, "N4itk: improved n3 bias correction," *IEEE transactions on medical imaging*, vol. 29, no. 6, pp. 1310–1320, 2010.

[11] B. B. Avants, C. L. Epstein, M. Grossman, and J. C. Gee, "Symmetric diffeomorphic image registration with cross-correlation: evaluating automated labeling of elderly and neurodegenerative brain," *Medical image analysis*, vol. 12, no. 1, pp. 26–41, 2008.

[12] Y. Zhang, M. Brady, and S. Smith, "Segmentation of brain mr images through a hidden markov random field model and the expectation-maximization algorithm," *IEEE Transactions on Medical Imaging*, vol. 20, no. 1, pp. 45–57, 2001.

[13] A. M. Dale, B. Fischl, and M. I. Sereno, "Cortical surface-based analysis: I. segmentation and surface reconstruction," *Neuroimage*, vol. 9, no. 2, pp. 179–194, 1999.

[14] A. Klein, S. S. Ghosh, F. S. Bao, J. Giard, Y. Häme, E. Stavsky, N. Lee, B. Rossa, M. Reuter, E. Chaibub Neto, *et al.*, "Mindboggling morphometry of human brains," *PLoS computational biology*, vol. 13, no. 2, p. e1005350, 2017.

[15] V. S. Fonov, A. C. Evans, R. C. McKinstry, C. Almli, and D. Collins, "Unbiased nonlinear average age-appropriate brain templates from birth to adulthood," *NeuroImage*, no. 47, p. S102, 2009.

[16] B. T. Yeo, F. M. Krienen, J. Sepulcre, M. R. Sabuncu, D. Lashkari, M. Hollinshead, J. L. Roffman, J. W. Smoller, L. Zöllei, J. R. Polimeni, *et al.*, "The organization of the human cerebral cortex estimated by intrinsic functional connectivity," *Journal of neurophysiology*, 2011.

[17] J. L. Vincent, I. Kahn, A. Z. Snyder, M. E. Raichle, and R. L. Buckner, "Evidence for a frontoparietal control system revealed by intrinsic functional connectivity," *Journal of neurophysiology*, vol. 100, no. 6, pp. 3328–3342, 2008.

[18] M. D. Fox, M. Corbetta, A. Z. Snyder, J. L. Vincent, and M. E. Raichle, "Spontaneous neuronal activity distinguishes human dorsal and ventral attention systems," *Proceedings of the National Academy of Sciences*, vol. 103, no. 26, pp. 10046–10051, 2006.

[19] R. W. Cox, "Afni: software for analysis and visualization of functional magnetic resonance neuroimages," *Computers and Biomedical research*, vol. 29, no. 3, pp. 162–173, 1996.

[20] D. N. Greve and B. Fischl, "Accurate and robust brain image alignment using boundary-based registration," *Neuroimage*, vol. 48, no. 1, pp. 63–72, 2009.

[21] M. Jenkinson, P. Bannister, M. Brady, and S. Smith, "Improved optimization for the robust and accurate linear registration and motion correction of brain images," *Neuroimage*, vol. 17, no. 2, pp. 825–841, 2002.

[22] R. Ciric, A. F. Rosen, G. Erus, M. Cieslak, A. Adebimpe, P. A. Cook, D. S. Bassett, C. Davatzikos, D. H. Wolf, and T. D. Satterthwaite, "Mitigating head motion artifact in functional connectivity mri," *Nature protocols*, vol. 13, no. 12, pp. 2801–2826, 2018.

[23] A. Abraham, F. Pedregosa, M. Eickenberg, P. Gervais, A. Mueller, J. Kossaifi, A. Gramfort, B. Thirion, and G. Varoquaux, "Machine learning for neuroimaging with scikit-learn," *Frontiers in neuroinformatics*, vol. 8, p. 14, 2014.

[24] D. Cosme, J. Flournoy, and K. DeStasio, "dsnlab/auto-motion: In house," May 2018.

[25] R. W. Cox, G. Chen, D. R. Glen, R. C. Reynolds, and P. A. Taylor, "Fmri clustering in afni: false-positive rates redux," *Brain connectivity*, vol. 7, no. 3, pp. 152–171, 2017.

[26] J. Veraart, D. S. Novikov, D. Christiaens, B. Ades-Aron, J. Sijbers, and E. Fieremans, "Denoising of diffusion mri using random matrix theory," *Neuroimage*, vol. 142, pp. 394–406, 2016.

[27] E. Kellner, B. Dhital, V. G. Kiselev, and M. Reisert, "Gibbs-ringing artifact removal based on local subvoxel-shifts," *Magnetic resonance in medicine*, vol. 76, no. 5, pp. 1574–1581, 2016.

[28] J. L. Andersson and S. N. Sotiropoulos, "An integrated approach to correction for off-resonance effects and subject movement in diffusion mr imaging," *Neuroimage*, vol. 125, pp. 1063–1078, 2016.

[29] J. L. Andersson, S. Skare, and J. Ashburner, "How to correct susceptibility distortions in spin-echo echo-planar images: application to diffusion tensor imaging," *Neuroimage*, vol. 20, no. 2, pp. 870–888, 2003.

[30] J. D. Power, A. Mitra, T. O. Laumann, A. Z. Snyder, B. L. Schlaggar, and S. E. Petersen, "Methods to detect, characterize, and remove motion artifact in resting state fmri," *Neuroimage*, vol. 84, pp. 320–341, 2014.

[31] E. Garyfallidis, M. Brett, B. Amirbekian, A. Rokem, S. Van Der Walt, M. Descoteaux, and I. Nimmo-Smith, "Dipy, a library for the analysis of diffusion mri data," *Frontiers in neuroinformatics*, vol. 8, p. 8, 2014.

[32] J. Peirce, J. R. Gray, S. Simpson, M. MacAskill, R. Höchenberger, H. Sogo, E. Kastman, and J. K. Lindeløv, "Psychopy2: Experiments in behavior made easy," *Behavior research methods*, vol. 51, no. 1, pp. 195–203, 2019.

[33] E. López-Caneda and C. Carbia, "The galician beverage picture set (gbps): A standardized database of alcohol and non-alcohol images," *Drug and alcohol dependence*, vol. 184, pp. 42–47, 2018.

[34] T. Babor, J. Higgins-Biddle, J. Saunders, and M. Monteiro, "Audit. the alcohol use disorders test. guidelines for use in primary care," *World Health Organization. Department of Mental Health and Substance Dependence*, 2001.

[35] M. M. Bradley and P. J. Lang, "Measuring emotion: the self-assessment manikin and the semantic differential," *Journal of behavior therapy and experimental psychiatry*, vol. 25, no. 1, pp. 49–59, 1994.

[36] Y. Kang, J. Gruber, and J. R. Gray, "Mindfulness and de-automatization," *Emotion review*, vol. 5, no. 2, pp. 192–201, 2013.

[37] C. Westbrook, J. D. Creswell, G. Tabibnia, E. Julson, H. Kober, and H. A. Tindle, "Mindful attention reduces neural and self-reported cue-induced craving in smokers," *Social cognitive and affective neuroscience*, vol. 8, no. 1, pp. 73–84, 2013.

[38] H. Kober, J. Buhle, J. Weber, K. N. Ochsner, and T. D. Wager, "Let it be: mindful acceptance down-regulates pain and negative emotion," *Social cognitive and affective neuroscience*, vol. 14, no. 11, pp. 1147–1158, 2019.

[39] E. C. Nook, A. B. Satpute, and K. N. Ochsner, "Emotion naming impedes both cognitive reappraisal and mindful acceptance strategies of emotion regulation," *Affective Science*, vol. 2, no. 2, pp. 187–198, 2021.

[40] A. Lutz, H. A. Slagter, J. D. Dunne, and R. J. Davidson, "Attention regulation and monitoring in meditation," *Trends in cognitive sciences*, vol. 12, no. 4, pp. 163–169, 2008.

[41] A. Chiesa, A. Serretti, and J. C. Jakobsen, "Mindfulness: Top–down or bottom–up emotion regulation strategy?," *Clinical psychology review*, vol. 33, no. 1, pp. 82–96, 2013.

[42] M. Corbetta and G. L. Shulman, "Control of goal-directed and stimulus-driven attention in the brain," *Nature reviews neuroscience*, vol. 3, no. 3, pp. 201–215, 2002.

[43] H. Y. Weng, J. A. Lewis-Peacock, F. M. Hecht, M. R. Uncapher, D. A. Ziegler, N. A. Farb, V. Goldman, S. Skinner, L. G. Duncan, M. T. Chao, *et al.*, "Focus on the breath: Brain decoding reveals internal states of attention during meditation," *Frontiers in human neuroscience*, p. 336, 2020.

[44] T. D. Wager and L. Y. Atlas, "The neuroscience of placebo effects: connecting context, learning and health," *Nature Reviews Neuroscience*, vol. 16, no. 7, pp. 403–418, 2015.

[45] S. Geuter, L. Koban, and T. D. Wager, "The cognitive neuroscience of placebo effects: concepts, predictions, and physiology," *Annu Rev Neurosci*, vol. 40, no. 1, pp. 167–188, 2017.

[46] M. Jovanova, D. Cosme, B. Doré, Y. Kang, O. Stanoi, N. Cooper, C. Helion, S. Lomax, P. McGowan, Amanda L, Z. M. Boyd, and et al., "Psychological distance intervention reminders reduce alcohol consumption frequency in daily life," May 2022.

[47] E. K. Papies, L. W. Barsalou, and R. Custers, "Mindful attention prevents mindless impulses," *Social Psychological and Personality Science*, vol. 3, no. 3, pp. 291–299, 2012.

[48] E. K. Papies, T. M. Pronk, M. Keesman, and L. W. Barsalou, "The benefits of simply observing: mindful attention modulates the link between motivation and behavior.," *Journal of Personality and Social Psychology*, vol. 108, no. 1, p. 148, 2015.

[49] L. A. Lebois, E. K. Papies, K. Gopinath, R. Cabanban, K. S. Quigley, V. Krishnamurthy, L. F. Barrett, and L. W. Barsalou, "A shift in perspective: Decentering through mindful attention to imagined stressful events," *Neuropsychologia*, vol. 75, pp. 505–524, 2015.

[50] D. M. Fresco, M. T. Moore, M. H. van Dulmen, Z. V. Segal, S. H. Ma, J. D. Teasdale, and J. M. G. Williams, "Initial psychometric properties of the experiences questionnaire: validation of a self-report measure of decentering," *Behavior therapy*, vol. 38, no. 3, pp. 234–246, 2007.

[51] D. C. Atkins, S. A. Baldwin, C. Zheng, R. J. Gallop, and C. Neighbors, "A tutorial on count regression and zero-altered count models for longitudinal substance use data.," *Psychology of Addictive Behaviors*, vol. 27, no. 1, p. 166, 2013.

[52] M. E. Brooks, K. Kristensen, K. J. Van Benthem, A. Magnusson, C. W. Berg, A. Nielsen, H. J. Skaug, M. Machler, and B. M. Bolker, "glmmtmb balances speed and flexibility among packages for zero-inflated generalized linear mixed modeling," *The R journal*, vol. 9, no. 2, pp. 378–400, 2017.

[53] J. L. Maggs, L. R. Williams, and C. M. Lee, "Ups and downs of alcohol use among first-year college students: Number of drinks, heavy drinking, and stumble and pass out drinking days," *Addictive behaviors*, vol. 36, no. 3, pp. 197–202, 2011.

[54] J. W. LaBrie, J. F. Hummer, and E. R. Pedersen, "Reasons for drinking in the college student context: The differential role and risk of the social motivator," *Journal of studies on alcohol and drugs*, vol. 68, no. 3, pp. 393–398, 2007.

[55] Y. Kang, N. Cooper, P. Pandey, C. Scholz, M. B. O'Donnell, M. D. Lieberman, S. E. Taylor, V. J. Strecher, S. Dal Cin, S. Konrath, *et al.*, "Effects of self-transcendence on neural responses to persuasive messages and health behavior change," *Proceedings of the National Academy of Sciences*, vol. 115, no. 40, pp. 9974–9979, 2018.

[56] A. J. Vickers and D. G. Altman, "Analysing controlled trials with baseline and follow up measurements," *Bmj*, vol. 323, no. 7321, pp. 1123–1124, 2001.

[57] M. M. Glymour, J. Weuve, L. F. Berkman, I. Kawachi, and J. M. Robins, "When is baseline adjustment useful in analyses of change? an example with education and cognitive change," *American journal of epidemiology*, vol. 162, no. 3, pp. 267–278, 2005.

[58] S. E. Gilman, J. Breslau, K. J. Conron, K. C. Koenen, S. Subramanian, and A. Zaslavsky, "Education and race-ethnicity differences in the lifetime risk of alcohol dependence," *Journal of Epidemiology & Community Health*, vol. 62, no. 3, pp. 224–230, 2008.

[59] R. Rojiani, J. F. Santoyo, H. Rahrig, H. D. Roth, and W. B. Britton, "Women benefit more than men in response to college-based meditation training," *Frontiers in psychology*, vol. 8, p. 551, 2017.

[60] Y. Kang, H. Rahrig, K. Eichel, H. F. Niles, T. Rocha, N. E. Lepp, J. Gold, and W. B. Britton, "Gender differences in response to a school-based mindfulness training intervention for early adolescents," *Journal of school psychology*, vol. 68, pp. 163–176, 2018.

[61] C. Schnohr, L. Højbjerre, M. Riegels, L. Ledet, T. Larsen, K. Schultz-Larsen, L. Petersen, E. Prescott, and M. Grønbæk, "Does educational level influence the effects of smoking, alcohol, physical activity, and obesity on mortality? a prospective population study," *Scandinavian journal of public health*, vol. 32, no. 4, pp. 250–256, 2004.

[62] B. Borsari, J. G. Murphy, and N. P. Barnett, "Predictors of alcohol use during the first year of college: Implications for prevention," *Addictive behaviors*, vol. 32, no. 10, pp. 2062–2086, 2007.

[63] K. Chartier and R. Caetano, "Ethnicity and health disparities in alcohol research," *Alcohol Research & Health*, vol. 33, no. 1-2, p. 152, 2010.

[64] P. P. Lui, S. R. Berkley, and B. L. Zamboanga, "College alcohol belief and alcohol use: Testing moderations by cultural orientations and ethnicity.," *Journal of counseling psychology*, vol. 67, no. 2, p. 184, 2020.

[65] K. W. Brown and R. M. Ryan, "The benefits of being present: mindfulness and its role in psychological well-being.," *Journal of personality and social psychology*, vol. 84, no. 4, p. 822, 2003.

[66] Y.-Y. Tang, B. K. Hölzel, and M. I. Posner, "The neuroscience of mindfulness meditation," *Nature Reviews Neuroscience*, vol. 16, no. 4, pp. 213–225, 2015.

[67] K. L. Gratz and L. Roemer, "Multidimensional assessment of emotion regulation and dysregulation: Development, factor structure, and initial validation of the difficulties in emotion regulation scale," *Journal of psychopathology and behavioral assessment*, vol. 26, no. 1, pp. 41–54, 2004.

[68] R. S. Desikan, F. Ségonne, B. Fischl, B. T. Quinn, B. C. Dickerson, D. Blacker, R. L. Buckner, A. M. Dale, R. P. Maguire, B. T. Hyman, *et al.*, "An automated labeling system for subdividing the human cerebral cortex on mri scans into gyral based regions of interest," *Neuroimage*, vol. 31, no. 3, pp. 968–980, 2006.

[69] T. M. Karrer, J. Z. Kim, J. Stiso, A. E. Kahn, F. Pasqualetti, U. Habel, and D. S. Bassett, "A practical guide to methodological considerations in the controllability of structural brain networks," *Journal of neural engineering*, vol. 17, no. 2, p. 026031, 2020.

[70] S. Gu, F. Pasqualetti, M. Cieslak, Q. K. Telesford, B. Y. Alfred, A. E. Kahn, J. D. Medaglia, J. M. Vettel, M. B. Miller, S. T. Grafton, *et al.*, "Controllability of structural brain networks," *Nature communications*, vol. 6, p. 8414, 2015.

[71] P. Srivastava, E. Nozari, J. Z. Kim, H. Ju, D. Zhou, C. Becker, F. Pasqualetti, G. J. Pappas, and D. S. Bassett, "Models of communication and control for brain networks: distinctions, convergence, and future outlook," *Network Neuroscience*, vol. 4, no. 4, pp. 1122–1159, 2020.

[72] R. F. Betzel, S. Gu, J. D. Medaglia, F. Pasqualetti, and D. S. Bassett, "Optimally controlling the human connectome: the role of network topology," *Scientific reports*, vol. 6, no. 1, pp. 1–14, 2016.

[73] E. J. Cornblath, E. Tang, G. L. Baum, T. M. Moore, A. Adebimpe, D. R. Roalf, R. C. Gur, R. E. Gur, F. Pasqualetti, T. D. Satterthwaite, and D. S. Bassett, "Sex differences in network controllability as a predictor of executive function in youth," *NeuroImage*, vol. 188, pp. 122–134, 2019.

[74] E. J. Cornblath, A. Ashourvan, J. Z. Kim, R. F. Betzel, R. Ciric, A. Adebimpe, G. L. Baum, X. He, K. Ruparel, T. M. Moore, *et al.*, "Temporal sequences of brain activity at rest are constrained by white matter structure and modulated by cognitive demands," *Communications biology*, vol. 3, no. 1, pp. 1–12, 2020.

[75] A. S. Mahadevan, E. J. Cornblath, D. M. Lydon-Staley, D. J. Zhou, L. M. Parkes, B. Larsen, A. Adebimpe, A. E. Kahn, R. C. Gur, R. E. Gur, *et al.*, "Alprazolam modulates persistence energy during emotion processing in first-degree relatives of individuals with schizophrenia: a network control study," *bioRxiv*, 2021.

[76] D. Cosme, "*NeuroVault.* statistical maps." `https://neurovault.org/collections/QCJQYFVZ/download`. Deposited 22 August 2022.

[77] Y. Kang, D. Cosme, D. Lydon-Staley, J. Ahn, M. Jovanova, F. Corbani, S. Lomax, O. Stanoi, V. Strecher, P. J. Mucha, *et al.*, "Purpose in life, neural alcohol cue reactivity, and daily alcohol use in social drinkers," *Addiction*.

[78] A. C. Lim, R. Green, E. N. Grodin, A. Venegas, L. R. Meredith, S. Donato, E. Burnette, and L. A. Ray, "Alcohol cue–induced ventral striatum activity predicts subsequent alcohol self-administration," *Alcoholism: Clinical and Experimental Research*, vol. 44, no. 6, pp. 1224–1233, 2020.

[79] D. Karl, J. M. Bumb, P. Bach, C. Dinter, A. Koopmann, D. Hermann, K. Mann, F. Kiefer, and S. Vollstädt-Klein, "Nalmefene attenuates neural alcohol cue-reactivity in the ventral striatum and subjective alcohol craving in patients with alcohol use disorder," *Psychopharmacology*, vol. 238, no. 8, pp. 2179–2189, 2021.

[80] T. Yarkoni, R. A. Poldrack, T. E. Nichols, D. C. Van Essen, and T. D. Wager, "Large-scale automated synthesis of human functional neuroimaging data," *Nature methods*, vol. 8, no. 8, pp. 665–670, 2011.

[81] L. Weninger, P. Srivastava, D. Zhou, J. Z. Kim, E. J. Cornblath, M. A. Bertolero, U. Habel, D. Merhof, and D. S. Bassett, "The information content of brain states is explained by structural constraints on state energetics," *arXiv preprint arXiv:2110.13781*, 2021.

[82] N. Tzourio-Mazoyer, B. Landeau, D. Papathanassiou, F. Crivello, O. Etard, N. Delcroix, B. Mazoyer, and M. Joliot, "Automated anatomical labeling of activations in spm using a macroscopic anatomical parcellation of the mni mri single-subject brain," *Neuroimage*, vol. 15, no. 1, pp. 273–289, 2002.

[83] R. V. Raut, A. Z. Snyder, and M. E. Raichle, "Hierarchical dynamics as a macroscopic organizing principle of the human brain," *Proceedings of the National Academy of Sciences*, vol. 117, no. 34, pp. 20890–20897, 2020.

[84] R. Gao, R. L. van den Brink, T. Pfeffer, and B. Voytek, "Neuronal timescales are functionally dynamic and shaped by cortical microarchitecture," *Elife*, vol. 9, p. e61277, 2020.